Solution of the asymmetric double sine-Gordon equation

Nan-Hong Kuo[1], Sujit Sarkar[2], C. D. Hu[1,3]

[1]Department of physics, National Taiwan University, Taipei, Taiwan, R.O.C.

[2]Poornaprajna Institute of Scientific Research, 4 Sadashivanagar, Bangalore-560 080, India.

[3]Center for Theoretical Sciences, National Taiwan University, Taipei, Taiwan, R.O.C.

Abstract

We present solutions of asymmetric double sine-Gordon equation (DSGE) of an infinite system based on Möbius transformation and numerical exercise. This method is able to give the forms of the solutions for all the region on the $\varphi - \eta$ parameter plane where φ is an additional phase and η is the ratio of the magnitudes of two sine terms. We are able to show how the deconfinement occurs near $\varphi = (1/2 + n)\pi$ and $\varphi = n\pi$. and also find the solution for all values of φ. We predict different kind of solutions and transitions among them in different parts of the parameter space of this equation.

0.0.1 1. Introduction:

The sine-Gordon equation attracted much interest of physicists[1,2]. In quantum field theory it is a rare example of integrable system which can be a starting point of developing non-perturbative theory. It also has plenty of application in condensed matter systems[3,4] and nonlinear optics[5]. However, the Lagrangian of a realistic physical system often gives a more complicated equation of motion than the sine-Gordon equation. For example, a quantum spin chain is mapped into a Lagrangian with several potential terms[6]. Systems with nonlinear optical properties also give rise to more complicated wave equations[7]. Thus a more complete model is desirable. This leads to the double sine-Gordon equation (DSGE) and loses the integrability of the sine-Gordon equation. But this "flaw" also provides a test ground for various analysis[8-11] and perturbative or non-perturbative methods such as form factor perturbation theory[12,13],.truncated conformal space approach[13,14] and semiclassical approach[15]. For a standard DSGE, exact solutions can be found[8,10]. But for a asymmetric DSGE

$$\theta_{tt} - \theta_{xx} + \sin(\theta + \varphi) + 2\eta \sin 2\theta = 0. \tag{1}$$

with φ being an additional phase, exact solution has eluded the effort of researchers. It is interesting not only because the state equations of a strongly correlated electron system[16], a quantum spin chain with external field or that of a spin pump[17,18] can be mapped into eq. (1) but from a purely theoretical point of view, it contain rich physics as we shall see.

The main difficulty of DSGE is that it is non-integrable. A rigorous analytical form of the solutions of asymmetric DSGE is important because it can provide deeper insight to understand the physical systems. It is also well known that the perturbation theory is not applicable in one-dimension because there is no quasi-particle excitation alike in higher dimension. Various approximation methods, perturbative or non-perturbative, sometimes give results leading to different physical pictures[14]. For this reasons, we would not like to solve this equation with above methods. We propose an insightful analytical form of the solution which can serve as an anchor to numerical analysis or approximations. It can also be a springboard to study quantum fluctuations.

The plan of the manuscript is the following: In Section **2**, we present previously existed classical solutions of DSGE depend on the potential coefficient η. We also present explicitly shortcomings of these analytical solutions. Section **3** contains the major part of our work. We present mathematical solution we find with Möbius transformation and see how parameters change with η and φ. In Section **4**, We present results and discussions.

0.0.2 2. Classical solutions of Double Sine-Gordon Equation

In this section, we briefly review the previously existed solutions in the literature, potential and energy of the double sine-Gordon equation (DSGE) with $\varphi = 0$ in order to establish the notations and set the stage for developing our method. We shall use the notations of ref. 4 and also point out the shortcoming of that

work. As mentioned in ref. 4, the Hamiltonian of the DSGE can be viewed as a chain of physical pendulums joined by torsion springs

$$H = \int dx \{ \frac{p_\theta^2}{2I} + \frac{\Gamma}{2}\theta_x^2 - V_0[\cos\theta + \eta\cos 2\theta] \} \tag{2}$$

where θ is the angular coordinate, p_θ is the conjugate momentum, I is the moment of inertia, Γ is the torsional constant, and V_0 is the external potential. The DSGE which we are interested in (eq. (1).) can be obtained with rescalings of the time-space coordinates. In order to calculate the total energy, one can Integrate both sides of eq. (1) and get

$$\frac{1}{2}(\frac{d\theta}{ds})^2 + \cos(\theta+\varphi) + \eta\cos(2\theta) = S \tag{3}$$

where $s = \gamma(x - vt)$, $\gamma = 1/\sqrt{1-v^2}$ and ν is the velocity of soliton. The negative sum of the last two terms can be viewed as the potential

$$V(\theta;\eta,\varphi) = -\cos(\theta+\varphi) - \eta\cos(2\theta) \tag{4}$$

and so S is called the "action". We can show that

$$S = -V_{\min}. \tag{5}$$

The solutions of kinks and bubbles (see ref. 4 and/or eqs. (28), (35) and (37) below) approach constant when $s \to \pm\infty$. Hence, $d\theta/ds|_{s=\pm\infty} = 0$ and $S = -V(\theta(\pm\infty))$. Since $(d\theta/ds)^2/2 = V(\theta) - V(\theta(\pm\infty)) \geq 0$ for any s, we conclude that $S = -V(\theta(\pm\infty)) = -V_{\min}$. More specifically, whether the minimum is an absolute minimum or a relative minimum depends on what type of the solution is.

Now we would like to calculate energy for all φ. The calculation of energy can be performed with the a method similar to that of ref. 2. We get from eq. 3. that

$$\frac{d\theta}{ds} = \sqrt{2[S - \cos(\theta+\varphi) - \eta\cos 2\theta]}. \tag{6}$$

We define

$$V_s \equiv \int_{-\infty}^{\infty} [\frac{\theta_x^2}{2} + \frac{\theta_t^2}{2}]dx = (1+v^2)\gamma \int_{-\infty}^{\infty} \frac{\theta_s^2}{2} ds = \frac{(1+v^2)\gamma}{\sqrt{2}} \int_0^{2\pi} \sqrt{S - \cos(\theta+\varphi) - \eta\cos 2\theta} d\theta \tag{7}$$

and

$$V_p \equiv \int_{-\infty}^{\infty} [-\cos(\theta+\varphi) - \eta\cos 2\theta]dx = \frac{1}{\gamma}\int_{-\infty}^{\infty} [-\cos(\theta+\varphi) - \eta\cos 2\theta]ds. \tag{8}$$

so that $H = V_s + V_p$ with some scaling. From eq. (3) we found that

$$V_p = -\frac{S \cdot s|_{s=0}^{s=L}}{\gamma} + \frac{1}{\gamma}\int_{-\infty}^{\infty} \frac{\theta_s^2}{2} ds. \tag{9}$$

But the first term on the right hand side of eq. (8) diverges if we consider an infinite system ($L \to \infty$). Thus we subtract this trivial infinity from the Hamiltonian in eq. (2). This is equivalent to shift the system to a new energy zero. In view of eq. (2), we get

$$H = V_s + V_p = 2\gamma \int_{-\infty}^{\infty} \frac{\theta_s^2}{2} ds. \tag{10}$$

While solving for solutions, we can obtain numerical values of S. Hence, the energy at every φ can be calculated.

An analysis of the potential term is in order. It helps us to understand how state evolves with respect to the phase φ. The potential of double sine-Gordon equation has the symmetry

$$V(\theta; \eta, \varphi = \frac{\pi}{2}) = V(\widetilde{\theta}; -\eta, \varphi = 0) \tag{11}$$

where $\widetilde{\theta} = \theta + \pi/2$. This implies that the solution of $\varphi = \pi/2$ has the same form as that of $\varphi = 0$ and $-\eta$. However, interestingly, the solutions can have completely different forms for $\varphi = 0$ or $\varphi = \pi/2$ when $|\eta| > \frac{1}{4}$ (see below).

In view of eq. (4), we have

$$\begin{aligned}\frac{dV}{d\theta} &= \sin(\theta + \varphi) + 2\eta \sin(2\theta) \\ &= \sin\theta(\cos\varphi + \cot\theta \sin\varphi + 4\eta\cos\theta) \\ &= \cos\theta(\sin\varphi + \tan\theta\cos\varphi + 4\eta\sin\theta).\end{aligned}$$

The point $\theta = \cos^{-1}(-1/4\eta)$ is one of the absolute maxima only if $\varphi = 0$ and $\eta < -1/4$, and $\theta = \sin^{-1}(-1/4\eta)$ is one of the absolute minima only if $\varphi = \pi/2$ and $\eta > 1/4$. Moreover, for $\eta < -1/4$ the relative minima are at $\theta = \pi/2 + 2n\pi$ and for $\eta > 1/4$ the relative maxima are at $\theta = 2n\pi$. The shape of the potential has critical influence on the form of the solution. We show their features in Figures 1a˜1c versus θ for $\eta = -0.35$, $\eta = 0.15$ and $\eta = 0.35$ respectively. Notably, for $(\eta = -0.35, \varphi = \pi/2)$ and $(\eta = 0.35, \varphi = 0)$ there are relative minima and for $(\eta = -0.35, \varphi = 0)$ and $(\eta = 0.35, \varphi = \pi/2)$ there are relative maxima. Nevertheless, for $\eta = 0.15$, there is no relative extremum. In general, there is a region where no relative extremum exists. In the regions where relative extremum exist, a so called bubble solution can be found. Another symmetry can be seen by making transformation $\theta' = \theta + \varphi$, eq. (4) becomes $V(\theta; \eta, \varphi) = -\cos\theta' - \eta\cos(2\theta' - 2\varphi)$. This shows that there is a period of π for the variation of φ.

Specifically, when $\varphi = 0$ and $\varphi = \pi/2$ the analytical forms of solution and energy can be obtained. In order to set up our analysis, in the following we give a summary of the solutions and energies in the case $\varphi = 0$.

Case 1 $\eta < -\frac{1}{4}$

In this case the absolute minima are at $\theta_{abs.\min} = \varphi_0 + 2n\pi$ where

$$\varphi_0 \equiv \arccos(\frac{-1}{4\eta}). \tag{12}$$

From above, we have $S = -V(\theta_{\min}) = -\eta - 1/8\eta$. The absolute maximum of $V(\theta)$ are located at $\theta_{abs.\max} = (2n+1)\pi$ while the relative maximum are located at $\theta_{rel.\max} = 2n\pi$ with $V(\theta_{abs.\max}) = 1 - \eta$ and $V(\theta_{rel.\max}) = -1 - \eta$. There are two kinds of traveling kinks:

$$\theta^{>} = 2\arctan[\pm\sqrt{\frac{4|\eta|-1}{4|\eta|+1}}\coth(\sqrt{\frac{16\eta^2-1}{16|\eta|}}s)], \tag{13}$$

$$\theta^{<} = 2\arctan[\pm\sqrt{\frac{4|\eta|-1}{4|\eta|+1}}\tanh(\sqrt{\frac{16\eta^2-1}{16|\eta|}}s)] \tag{14}$$

where the superscripts $>$ and $<$ denote the large kink and small kink respectively. We discuss their energies separately.

(A) Large kink: We found from eq. (13) that $\theta \in [\varphi_0, 2\pi - \varphi_0]$, and it must vary cross one of the absolute maxima. In view of eqs. (7) and (10),

$$\begin{aligned}\langle H\rangle &= 2\gamma\int_{-\infty}^{\infty}\frac{\theta_s^2}{2}ds = \sqrt{2}\gamma\int_{\varphi_0}^{2\pi-\varphi_0}\sqrt{-\eta-\frac{1}{8\eta}-\cos\theta-\eta\cos 2\theta d\theta} = \sqrt{2}\gamma\int_{\varphi_0}^{2\pi-\varphi_0}\sqrt{-2\eta(\cos\theta+\frac{1}{4\eta})^2 d\theta} \\ &= \frac{\gamma}{\sqrt{-\eta}}(\sqrt{16\eta^2-1}+\pi-\varphi_0) \end{aligned}\tag{15}$$

(B) Small kink: From eq. (14) we found that $\theta \in [-\varphi_0, \varphi_0]$, and it must contain one of the relative maxima

$$\langle H\rangle = 2\gamma\int_{-\infty}^{\infty}\frac{\theta_s^2}{2}ds = \sqrt{2}\gamma\int_{\varphi_0}^{-\varphi_0}\sqrt{-\eta-\frac{1}{8\eta}-\cos\theta-\eta\cos 2\theta d\theta} = \frac{\gamma}{\sqrt{-\eta}}(\sqrt{16\eta^2-1}-\varphi_0) \tag{16}$$

Here, we have corrected the errors in eqs.(3.10) and (3.11) of ref. 4.

Case 2 $|\eta| < \frac{1}{4}$

There is only one type of basic kink solution in this case:

$$\theta^{>} = 2\arctan[\pm\sqrt{1+4\eta}csch(\sqrt{1+4\eta}s)] \tag{17}$$

The minimum of $V(\theta)$ are located at $\theta_{\min} = 2n\pi$ with $V(\theta_{\min}) = -1 - \eta$ and the maximum of $V(\theta)$ are located at $\theta_{\max} = (2n+1)\pi$ with $V(\theta_{\max}) = 1 - \eta$. There is no relative maximum or minimum. We have $S = -V(\theta_{\min}) = 1 + \eta$ and from eqs. (6) and (9),

$$\langle H\rangle = 2\gamma\int_{-\infty}^{\infty}\frac{\theta_s^2}{2}ds = \sqrt{2}\gamma\int_{0}^{2\pi}\sqrt{1+\eta-\cos\theta-\eta\cos 2\theta}d\theta \tag{18}$$

The integral also depends on wether η is larger or smaller than 0.

(A) $\frac{1}{4} > \eta > 0$

$$\langle H\rangle = 2\gamma\int_{-\infty}^{\infty}\frac{\theta_s^2}{2}ds = 4\gamma\sqrt{4\eta+1} + \frac{2\gamma\ln(2\sqrt{\eta}+\sqrt{4\eta+1})}{\sqrt{\eta}} \tag{19}$$

(B) $0 > \eta > -\frac{1}{4}$

$$\langle H \rangle = 2\gamma \int_{-\infty}^{\infty} \frac{\theta_s^2}{2} ds = 4\gamma\sqrt{4\eta + 1} + \frac{2\gamma \arcsin(2\sqrt{-\eta})}{\sqrt{-\eta}} \tag{20}$$

Here we have corrected an error in eq. (3.7) of ref. 4.

Case 3 $\eta > \frac{1}{4}$

There are two kinds of traveling kinks:

$$\theta^{>} = 2\arctan[\pm\sqrt{1+4\eta}csch(\sqrt{1+4\eta}s)], \tag{21}$$

and

$$\theta^{B} = 2\arctan[\pm\frac{1}{\sqrt{4\eta - 1}}\cosh(\sqrt{4\eta - 1}s)] \tag{22}$$

where the superscript B denotes the bubble solution. The absolute minimum of $V(\theta)$ are located at $\theta_{abs.\min} = 2n\pi$ with $V(\theta_{abs.\min}) = -1-\eta$ and the maximum of $V(\theta)$ are located at $\theta_{\max} = \arccos(-1/4\eta)+2n\pi$ with $V(\theta_{abs.\max}) = 1/8\eta+\eta$. The energy of the large kink is the same as that in case 2:

$$\langle H \rangle = 2\gamma \int_{-\infty}^{\infty} \frac{\theta_s^2}{2} ds = 4\gamma\sqrt{4\eta + 1} + \frac{2\gamma \ln(2\sqrt{\eta} + \sqrt{4\eta+1})}{\sqrt{\eta}} \tag{23}$$

The other kind of solution is the bubble solution. It extends from one relative minimum to another. These minima are at $\theta_{rel\min} \to (2n+1)\pi$ as $s \to \pm\infty$. In this case, $S = -V(\theta_{rel,\min}) = \eta - 1$

$$\begin{aligned} \langle H \rangle = 2\gamma \int_{-\infty}^{\infty} \frac{\theta_s^2}{2} ds &= 2\sqrt{2}\gamma \int_{2\arctan(1/\sqrt{4\eta-1})}^{\pi} \sqrt{\eta - 1 - \cos\theta - \eta\cos 2\theta} d\theta \\ &= 4\gamma\sqrt{4\eta - 1} - \frac{4\gamma \ln(2\sqrt{\eta} + \sqrt{4\eta - 1})}{\sqrt{\eta}}. \end{aligned} \tag{24}$$

Note the upper bound and lower bound of the integral. We divide the bubble into two equal halves. The upper bound π is the relative minimum while the lower bound is the middle point of the bubble. It comes from $\theta^B(s=0) = 2\arctan[\pm(4\eta-1)^{-1/2}\cosh(\sqrt{4\eta-1}s)]|_{s=0} = \pm 2\arctan(1/\sqrt{4\eta-1})$. Here we also corrected the errors in eq.(3.7) and (3.9) of ref. 4.

Further insight can be gained by applying eq. (11). For example, if we start from $\varphi = 0$ and $\eta > \frac{1}{4}$, the solutions are the large kink in eq. (21) and bubble in eq. (22). When φ is changed adiabatically into $\pi/2$, the solutions become the large and small kinks in eqs. (13) and (14):

$$\theta^{>} = 2\arctan[\pm\sqrt{\frac{4|\eta| - 1}{4|\eta| + 1}}\coth(\sqrt{\frac{16\eta^2 - 1}{16|\eta|}}s)] - \frac{\pi}{2},$$

$$\theta^{<} = 2\arctan[\pm\sqrt{\frac{4|\eta| - 1}{4|\eta| + 1}}\tanh(\sqrt{\frac{16\eta^2 - 1}{16|\eta|}}s)] - \frac{\pi}{2}$$

with the additional term $-\pi/2$ coming from the difference between θ and $\widetilde{\theta}$. Therefore, the solutions can have quite different forms as φ varies. The interesting question is whether the solution evolve smoothly or they change abruptly.

0.0.3 3. Solutions in general

In previous studies of asymmetric DSGE, the solution can be found when $\varphi = 0$ or $\varphi = \pi/2$. Here, we present a method which enables us to find solutions for any value of φ. We propose that the solution of eq. (1) in general has the form

$$\theta = 2\arctan[f(s)]. \tag{25}$$

Then after substitution, we have the following equation

$$2(\frac{df}{ds})^2 = (S+\cos(\varphi)-\eta)f^4+2\sin(\varphi)f^3+(2S+6\eta)f^2+2\sin(\varphi)f+(E-\cos(\varphi)-\eta) \tag{26}$$

Above equation is similar to the differential equation of Jacobi elliptic functions (JEF) or hyperbolic functions except for the terms with the odd power of $f(s)$. However, for JEF, there is the "Möbius transformation" to change eq. (26) into the standard form. The details is given in Appendix. By letting $f(s) = (ag(s)+b)/(cg(s)+d)$ and choosing suitable coefficients, a, b, c, and d, it is possible to obtain the following form from eq. (26)

$$(\frac{dg}{ds})^2 = a_4 g^4 + a_2 g^2 + a_0. \tag{27}$$

In an infinite system with arbitrary value of φ, it is reasonable to use for $g(s)$ the hyperbolic functions which JEFs approach in the limit of modulus $k \to 1$:

$$f(s) = \frac{a\sinh(rs)+b}{c\sinh(rs)+d} \tag{28}$$

where r is a constant. One may also use the other hyperbolic function for this construction. Substituting eqs. (25) and (28) into eq. (26) and requiring the same scaling

$$(ad-bc)^2 = 1 \tag{29}$$

we have found the following equations by comparing the powers of sinh function

$$(a^2+c^2)^2S+(a^4-c^4)\cos\varphi+2ac(a^2+c^2)\sin\varphi+(-a^4+6a^2c^2-c^4)\eta = 0, \tag{30a}$$

$$\begin{aligned} 4(ab+cd)(a^2+c^2)S + 4(a^3b-c^3d)\cos\varphi \\ + 2(a^3d+3a^2bc+3ac^2d+bc^3)\sin\varphi \\ + [-4a^3b+6(2a^2cd+2abc^2)-4c^3d]\eta = 0, \end{aligned} \tag{30b}$$

$$
\begin{aligned}
[6a^2b^2 + 2(a^2d^2 + 4abcd + b^2c^2) + 6c^2d^2]S& \\
+ (6a^2b^2 - 6c^2d^2)\cos\varphi& \\
+ 6(a^2bd + ab^2c + acd^2 + bc^2d)\sin\varphi& \\
+ 6(-a^2b^2 + a^2d^2 + 4abcd + b^2c^2 - c^2d^2)\eta = 2r^2& \qquad (30c)
\end{aligned}
$$

$$
\begin{aligned}
4(ab + cd)(b^2 + d^2)S + 4(b^3a - d^3c)\cos\varphi +& \\
2(b^3c + 3b^2ad + 3bd^2c + ad^3)\sin\varphi +& \\
[-4b^3a + 6(2d^2ab + 2cdb^2) - 4d^3c]\eta = 0& \qquad (30d)
\end{aligned}
$$

$$
(b^2+d^2)^2S + (b^4-d^4)\cos\varphi + 2bd(b^2+d^2)\sin\varphi + (-b^4+6b^2d^2-d^4)\eta = 2r^2 \quad (30e)
$$

The simultaneous algebraic equations are solved to give the coefficients a, b, c, d, r and S. Thus, we can find solutions for any values of η and φ except for certain special cases with the form in eq. (28). In Table 1, 2 and 3 we give the values of the parameters for several values of η and φ. The crosses in Table 3 indicate that eq. (28) cannot give any solution under these conditions.

The special case for which the form in eq. (28) cannot give any solution is well-defined and very interesting, it occurs at $\varphi = \pi/2$ and $\eta > 1/4$. We also explain the cause of this forbidden solution by starting with the symmetry of the DSGE with additional phase. If one substitutes $\pi - \varphi$ for φ, then he can replace θ with $\pi - \theta$ and eq. (1) retains its original form. In view of eqs. (25) and (28), we have the following symmetry:

$$
\begin{array}{ccc}
\varphi & \rightarrow & \pi - \varphi \\
a & \rightarrow & -c \\
b & \rightarrow & d \\
c & \rightarrow & -a \\
d & \rightarrow & b \\
r & \rightarrow & r \\
S & \rightarrow & S
\end{array} . \qquad (31)
$$

In other words, when φ is changed into $\pi - \varphi$, the solution becomes $\pi - \theta$. Suppose we have, and indeed we have found, real solution of eqs. (30) for $\eta > 1/4$ with a, b, c and d being continuous with varying φ, then we must have $a = -c$ and $b = d$ at $\varphi = \pi/2$. Substituting these into eqs. (30), we get

$$
a^4(S - 1 + \eta) = 0, \qquad (32a)
$$

$$
a^2b^2 = \frac{r^2}{4S - 12\eta}, \qquad (32b)
$$

$$
b^4(S + 1 + \eta) = \frac{r^2}{2}, \qquad (32c)
$$

along with the scaling restriction from eq. (29)

$$
4a^2b^2 = 1. \qquad (33)
$$

Eq. (33) means $a \neq 0$, and so eq. (32a) implies $S + \eta = 1$. Inserting these into eqs. (32b) and (32c), we get

$$\frac{r^2}{1-4\eta} = 1. \tag{34}$$

Incompatibility results from eq. (32) if $\eta > 1/4$.

On the other hand, we can find a solution of distinctively different form at $\eta > 1/4$ and $\varphi = \pi/2$. Instead of $g(s) = \sinh(rs)$, we now have $g(s) = \tanh(rs)$ or $g(s) = \coth(rs)$

$$f(s) = \frac{a\sinh(rs) + b\cosh(rs)}{c\sinh(rs) + d\cosh(rs)}. \tag{35}$$

The algebraic equations are

$$(a^2+c^2)^2 S + (a^4-c^4)\cos\varphi + 2ac(a^2+c^2)\sin\varphi + (-a^4+6a^2c^2-c^4)\eta = 2r^2 \tag{36a}$$

$$\begin{aligned} 4(ab+cd)(a^2+c^2)S + 4(a^3b - c^3d)\cos\varphi \\ + 2(a^3d + 3a^2bc + 3ac^2d + bc^3)\sin\varphi \\ + [-4a^3b + 6(2a^2cd + 2abc^2) - 4c^3d]\eta = 0 \end{aligned} \tag{36b}$$

$$\begin{aligned} [6a^2b^2 + 2(a^2d^2 + 4abcd + b^2c^2) + 6c^2d^2]S \\ + (6a^2b^2 - 6c^2d^2)\cos\varphi \\ + 6(a^2bd + ab^2c + acd^2 + bc^2d)\sin\varphi \\ + 6(-a^2b^2 + a^2d^2 + 4abcd + b^2c^2 - c^2d^2)\eta = -4r^2 \end{aligned} \tag{36c}$$

$$\begin{aligned} 4(ab+cd)(b^2+d^2)S + 4(b^3a - d^3c)\cos\varphi + \\ 2(b^3c + 3b^2ad + 3bd^2c + ad^3)\sin\varphi + \\ [-4b^3a + 6(2d^2ab + 2cdb^2) - 4d^3c]\eta = 0 \end{aligned} \tag{36d}$$

$$(b^2+d^2)^2 S + (b^4-d^4)\cos\varphi + 2bd(b^2+d^2)\sin\varphi + (-b^4+6b^2d^2-d^4)\eta = 2r^2 \tag{36e}$$

along with eq. (29). Notice that the only difference is that the right hand sides of eqs.(36a) and (36c) are different from those of eqs. (30a) and (30c). As we pointed out in eq. (11), there is another symmetry in parameters: $(\eta, \varphi = \pi/2) \to (-\eta, \varphi = 0)$. Hence, above analysis is also applicable to the case $\eta = -1/4$ and $\varphi = 0$. In fact the solutions can be reduced to eqs. (13) and (14).

We plot the kink solutions in Fig. 2 for $\eta = 0.15$ and $\varphi = 0\tilde{}1.75\pi$. The solutions at $\eta = 0.35$ and $\varphi = 0\tilde{}0.5\pi$ and $\varphi = 0.5\pi\tilde{}\pi$ are shown in Fig. 3a and Fig. 3b respectively. The kinks for $\eta < 1/4$ (Fig. 2) change smoothly and retain their shapes as φ moves across $\pi/2$. The total change of θ, $\Delta\theta = \theta(s = \infty) - \theta(s = -\infty)$, is equal to 2π. This can also be deduced from eq. (28) by tracing the variation of θ with respect to s. On the other hand, the solutions for $\eta > 1/4$ (Fig. 3a and 3b) develop a second kink as φ approaches $\pi/2$. At

$\varphi = \pi/2$, the form in eq. (28) is no longer applicable. Eq. (35) has to be used and it gives a large kink and a small kinks which are the decedents of the connected kinks at $\varphi = \pi/2 - \varepsilon$ where ε is an infinitesimal positive number. Note also that the total change of θ of neither the large kink nor the small kink is equal to 2π, but rather the sum of them is. This can also be seen from eq. (35).

We here propose a classical explanation of the situation near $\varphi = \pi/2$. It is related to the minima of the potential. As we have argued in section 2, $d\theta/ds|_{s=\pm\infty} = 0$ and $V(\theta(\pm\infty)) = V_{\min}$. The solutions in eqs. (28) and (35) extend from one minimum to another. The kink comes from eq. (28) starts from one absolute minimum of the potential, passing through a major peak and ends at another absolute minimum. In the special case with the solutions coming from eq. (35), there are a large kink and a small kink. Both connect two absolute minima but the former passes a major peak of the potential and the latter passes a minor peak. The large kink extends from $\theta = 2\arctan((b-a)/(d-c))$ to $\theta = 2\arctan((b+a)/(d+c))$ and the small kink extend from $\theta = 2\arctan((b+a)/(d+c)$ to $\theta = 2\pi + 2\arctan((b-a)/(d-c))$. It is the emergence of additional symmetry in potential which gives rise to two absolute minima in the range of 2π which in turn, requires two solutions. We will elaborate more on this in next section.

Finally, we give the form of the bubble solution. Instead of eq. (28), we use

$$f(s) = \frac{a\cosh(rs) + b}{c\cosh(rs) + d} \tag{37}$$

and follow the same procedure, we are able to obtain the bubble solution, similar to that in eq. (22). Its shape is shown in Fig. 4. by the dashed line which connects two relative minima of potential. The bubble solution can be found only when the relative minima exist.

0.0.4 4. Discussion and conclusion

We summarize our results on the φ–η phase diagram in Fig. 5. The kink solution in eq. (28) can be found in any place except for those vertical lines. On the vertical lines, the form in eq. (35) prevails. Note that it corresponds to either $g(s) = \coth(rs)$ or $g(s) = \tanh(rs)$, which in turn, corresponds respectively to large kink or small kink. The bubble solution exist in the region above the upper dashed line or below the lower dashed line, i.e., the regions where relative minima exist.

The limiting case is also interesting. In the limit $\eta \to 0$, the solutions should be those of an ordinary sine-Gordon equation: $\theta = 4\arctan[\exp(s)] = 2\arctan[\csc h(-s)]$. It is compatible with the form in eq. (28). In the other limit, $\eta \to \infty$, one can write eq. (1) as

$$\frac{1}{4\eta}\frac{\partial^2\theta'}{\partial t^2} - \frac{1}{4\eta}\frac{\partial^2\theta}{\partial x^2} + \frac{1}{2\eta}\sin(\theta'/2 + \varphi) + \sin\theta' = 0. \tag{38}$$

where $\theta' = 2\theta$. The third term can be treated as a perturbation. The zeroth order of the solutions should be those of sine-Gordon equation with $\sin(2\theta)$:

$$\theta = 2\arctan[\exp(s')] \tag{39}$$

Here, $s' = 2\sqrt{\eta}s$, implying $r = 2\sqrt{\eta}$ in eq. (28) as $\eta \to \infty$. This is shown clearly by the Möbius transformation below.

Consider only the leading order terms of eqs. (30) for large η

$$(a^2 + c^2)^2 S + (-a^4 + 6a^2c^2 - c^4)\eta = 0, \tag{40a}$$

$$4(ab + cd)(a^2 + c^2)S + [-4a^3b + 6(2a^2cd + 2abc^2) - 4c^3d]\eta = 0, \tag{40b}$$

$$[6a^2b^2+2(a^2d^2+4abcd+b^2c^2)+6c^2d^2]S+6(-a^2b^2+a^2d^2+4abcd+b^2c^2-c^2d^2)\eta = 2r^2 \tag{40c}$$

$$4(ab + cd)(b^2 + d^2)S[-4b^3a + 6(2d^2ab + 2cdb^2) - 4d^3c]\eta = 0 \tag{40d}$$

$$(b^2 + d^2)^2 S + (-b^4 + 6b^2d^2 - d^4)\eta = 2r^2. \tag{40e}$$

It can be shown easily that none of a, b, c and d can be 0. Hence we can set $a = pc$ and $b = qd$ where p and q are just two ratio parameters. With the condition eq. (29), it can be shown further that $q = -p = \pm 1$ and $|cd| = 1/\sqrt{2}$. Now let $S = -\eta + \delta$ where $\delta = O(\eta^0)$ and substitute it into eq. (40e), one find that $\delta = 2r^2/d^4$. This implies that $b = \pm d = O(\sqrt[4]{\eta})$ and $a = \pm c = O(1/\sqrt[4]{\eta})$. We thus have shown that for finite η, solutions of the form of eq. (28) always exist (except for $(\eta < 1/4, \varphi = 0)$ and $(\eta > 1/4, \varphi = \pi/2)$) and their parameters a, b, c and d vary smoothly with η. Hence, the solution for finite η has the same form as that for $\eta = 0$.

The only places where there are phase transition are the ends of the vertical lines in Fig. 5, i.e., the points $(\varphi = n\pi, \eta = -1/4)$ and $(\varphi = (n+1/2)\pi, \eta = 1/4)$. Here, indeed the form of the solutions changes from that in eq. (28) into that in eq. (35) when the absolute value of η increases. Classically, this is a second-order phase transition. Its quantum fluctuation has also been well-studied[12-15].

There is another aspect we would like to investigate and that is varying φ across $\varphi = \pi/2$ for a fixed η. We plot in Figure 6a and 6b the energy as a function of φ with $\eta = 0.15$ and $\eta = 0.35$ respectively. One can immediately notice the behavior of energy near $\varphi = \pi/2 + n\pi$. For $\eta = 0.15$, the slope change is large but still smooth. For $\eta = 0.35$, though the energy remains continuous, the slope does not. This indicates that when $|\eta| < 1/4$ there is smooth crossover. But when $|\eta| > 1/4$ there is a second-order phase transition from the energy point of view. The solutions also show different behavior. In Fig. 2, the kinks vary smoothly across the point $\varphi = \pi/2$ at $\eta = 0.15$. For the solutions in Figs. 3 with $\eta = 0.35$, one finds that near $\varphi \approx \pi/2$, the shapes of the solutions are different from those at $\varphi = \pi/2$. The solutions are combination of two kinks though their forms are still that of eq. (28), i.e. , $g(x) = \sinh(rx)$. As a result the range of variation of θ is still 2π. and the topological charge is unity. When $\varphi = \pi/2$ the form of the kinks is that of eq. (35), i.e., $g(x) = \tanh(rx)$ or $g(x) = \coth(rs)$, the large or small kink solutions. It is the sum of ranges of variation of θ of the

two kinks which is equal to 2π, and thus the deconfinement. It is due to the emergence of the symmetry that both θ and $\pi-\theta$ are solutions. On the other hand, the solutions at $\varphi=\pi/2\pm\varepsilon$ where ε is a infinitesimal number, are very similar. Our numerical results also show that the coefficients a, b, c, d and S vary smoothly across the point $\varphi=\pi/2$, (not including the point $\varphi=\pi/2$.) Thus, the point $\varphi=\pi/2$ for $\eta>1/4$ is actually a singular point.

In this work, we used the method of "Möbius transformation" to solve the asymmetric DSGE. This method transformed the DSGE into a set of algebraic equations. Thus we are able to find the forms of the solutions for all the region on the $\varphi-\eta$ plane. The resulting forms of our solutions can serve as the basis of various methods, such as form factor perturbation theory, semi-classical method or a truncated conformal space approach to study quantum fluctuation.

This work is supported in part by NSC of Taiwan, ROC under the contract number NSC 95-2112-M-002-048-MY3. One of the authors, C. D. Hu would like to thank Chern Chyh-Hong for inspiring discussion.

0.0.5 Appendix: Introduction to Möbius transformation

By Jacobi elliptic function theory, one can transform the following equation:

$$(\frac{df}{ds})^2=\varphi(s)=A(f-f_0)(f-f_1)(f-f_2)(f-f_3), \tag{A-1}$$

where $\varphi(s)$ is a polynomial of s to the three or four power and f_0, f_1, f_2 and f_3 are the roots, into the standard form, i.e., only terms with even powers are present. The "Möbius transformation" has the form

$$f=\frac{a\zeta+b}{c\zeta+d}, \tag{A-2}$$

and so does every root

$$f_i=\frac{a\zeta_i+b}{c\zeta_i+d}. \tag{A-3}$$

If we take special values of a, b, c and d, we can obtain the form

$$f=\frac{f_3(f_1-f_0)*\zeta-f_1(f_3-f_0)}{(f_1-f_0)\zeta-(f_3-f_0)} \tag{A-4}$$

and eq. (A-1) becomes

$$(\frac{d\varsigma}{ds})^2=B(\varsigma-\beta_0)(\varsigma-\beta_1)(\varsigma-\beta_2)(\varsigma-\beta_3). \tag{A-5}$$

We set

$$\lambda=\frac{f_1-f_0}{f_1-f_2}\frac{f_3-f_2}{f_3-f_0}=\frac{\beta_1-\beta_0}{\beta_1-\beta_2}\frac{\beta_3-\beta_2}{\beta_3-\beta_0}, \tag{A-6}$$

so that eq. (A-5) becomes

$$(\frac{d\varsigma}{ds})^2=B\varsigma(\varsigma-1)(\lambda\varsigma-1) \tag{A-7}$$

here $B = A(f_3 - f_0)(f_2 - f_1)$. This is the standard form. But we can do further transform by setting $\varsigma = \xi^2$. So eq. (A-7) becomes the differential equation of Jacobi elliptic function:

$$(\frac{d\xi}{ds})^2 = \frac{B}{4}(\xi^2 - 1)(\lambda\xi^2 - 1). \tag{A-8}$$

Instead eqs. (A.4) and (A.8), we can take different transformation by mapping roots into $1, -1, 1/k$, and $-1/k$. So

$$\lambda = \frac{f_1 - f_0}{f_1 - f_2}\frac{f_3 - f_2}{f_3 - f_0} = \frac{\frac{1}{k} - 1}{\frac{1}{k} + 1}\frac{\frac{-1}{k} + 1}{\frac{-1}{k} - 1} = (\frac{1 - k}{1 + k})^2 \tag{A-9}$$

and eq. (A-1) becomes

$$(\frac{d\xi}{ds})^2 = B'(\xi^2 - 1)(k^2\xi^2 - 1) \tag{A-10}$$

There are more details to be solved such as how to deal with degenerate roots and how to further transform λ so that it is real and in the range $(0, 1)$ in order that eq. (A-8) and (A-10) are compatible with the Jacobi elliptic differential equation. But these are beyond the scope of this work.

References: [1] S. Coleman, Phys. Rev. **D 11**, 3424 (1975).

[2] V. E. Korepin and L. D. Faddev, Theor. Mat. Fiz. **25**, 147 (1975).

[3] A. O. Gogolin, A. A. Nersesyan and A. M. Tsvelik, 'Bosonization and Strongly Correlated Systems', Cambridge University Press (1998).

[4] T. Giamarchi, 'Quantum Physics in One Dimension', Oxford University Press (2004).

[5]. R. K. Bullough and P. J. Caudrey,'Solitons', Springer-Verlag Berlin Heidelberg (1980).

[6]. N. Nagaosa, 'Quantum Field Theory in Stongly Correlated Electronic Systems', Springer-Verlag, Berlin (1999).

[7] R. K. Bullough, J. Mod. Opt., **47**, 2029 (2000) and erratum, *idbd*, **48**, 747 (2001).

[8] C. A. Condat, R. A. Guyerand M. D. Miller, Phys. Rev. **B 27**, 474 (1983).

[9] D. C. Campbell, J. E. Schonfeld and C. A. Wingate, Physica **19 D**, 165 (1986).

[10] Zuntao Fu, et. al., Z. Naturforsch **60a**, 301 (2005).

[11] G. Delfino, G. Mussardo and P. Simonetti, Nucl. Phys. **B 473**,.469 (1996).

[12] G. Delfino and G. Mussardo Nucl. Phys. **B 516**,.675 (1998).

[13] Z. Bajnok, L. Palla and G. Takács, Nucl Phys. **B 687**,.189 (2000).

[14] G. Takács and F. Wagner, Nucl. Phys. **B 741**,.353 (2006).

[15] G. Mussardo, V. Riva and G. Sotkov, Nucl Phys. **B 687**,.189 (2004).

[16] M. Fabrizo, A. O. Gogolin and A. A. Nersesyan, Nucl. Phys. **B 580**, 647 (2000)

[17] R. Shindou, J. Phys. Soc. Jpn. **74**, 1214 (2005).
[18] Nan-Hong Kuo, Sujit Sarkar and C. D. Hu, ,arXiv:0809.2185v1 [cond-mat.str-el] (2008).

Figure cations: Fig. 1 Potential energy v.s. θ for $\varphi = 0$ and (a) $\eta = -0.35$, (b) $\eta = 0.15$ and (c) $\eta = 0.35$.

Fig. 2 Solutions form the form of eq. (28) for $\eta = 0.15$ and $\varphi = 0\tilde{}7\pi/8$.

Fig. 3a Solutions from the form of eq. (28) for $\eta = 0.35$ and $\varphi = 0\tilde{}\pi/2$. At $\varphi = \pi/2$, the solutions have the form of eq. (35) which gives large and small kinks.

Fig. 3b Solutions from the form of eq. (28) for $\eta = 0.35$ and $\varphi = \pi/2\tilde{}\pi$. At $\varphi = \pi/2$, the solutions have the form of eq. (35) which gives large and small kinks.

Fig 4. kink solution (in dashed line) and bubble solution (in solid line) for $\eta = 0.35$ and $\varphi = 0$. θ is in unit of π.

Fig. 5 Phase diagram on $\varphi - \eta$ plane. See text for explanation.

Fig. 6 The energy of the kink versus φ, (a) $\eta = 0.15$, (b) $\eta = 0.35$.

Table 1 List of a, b, c, d, r, S for eq. (28) for. $\varphi = 0$

$\eta\diagdown$	a	b	c	d	r	S
-0.25	$\times$	$\times$	$\times$	$\times$	$\times$	0.75
-0.15	0	0.795271	1.25743	0	± 0.532456	0.85
0	0	1	1	0	± 1	1
0.15	0	1.12468	0.88914	0	± 1.26491	1.15
0.25	0	1.18921	0.840896	0	± 1.41421	1.25
0.35	0	1.24467	0.803428	0	± 1.54919	1.35
0.45	0	1.29357	0.773055	0	1.67332	1.45

Table 2 List of a, b, c, d, r, S for eq. (28) for. $\varphi = \pi/4$

$\eta\diagdown$	a	b	c	d	r	S
-0.25	-0.466708	0.836099	0.712245	0.866693	± 1.26959	1.10092
-0.15	-0.460968	0.828478	0.7977	0.735676	± 1.1254	1.04093
0	-0.382683	0.92388	0.92388	0.382683	± 1	1
0.15	-0.238106	1.10602	0.890012	0.0656207	± 1.1254	1.04093
0.25	-0.173621	1.20406	0.833646	-0.0216328	± 1.26959	1.10092
0.35	-0.13299	1.2828	0.785775	-0.0600972	± 1.41323	1.17461
0.45	-0.106325	1.34854	0.74763	-0.0772086	± 1.54803	1.25625

Table 3 List of a, b, c, d, r, S for eq. (28) for. $\varphi = \pi/2$

$\eta\diagdown$	a	b	c	d	r	S
-0.25	-0.594604	0.840896	0.594604	0.840896	± 1.41421	1.25
-0.15	-0.628717	0.795271	0.628717	0.795271	± 1.26491	1.15
0	-0.707107	0.707107	0.707107	0.707107	± 1	1
0.15	-0.88914	0.562341	0.88914	0.562341	± 0.632456	0.85
0.25	$\times$	$\times$	$\times$	$\times$	$\times$	$\times$
0.35	$\times$	$\times$	$\times$	$\times$	$\times$	$\times$
0.45	$\times$	$\times$	$\times$	$\times$	$\times$	$\times$

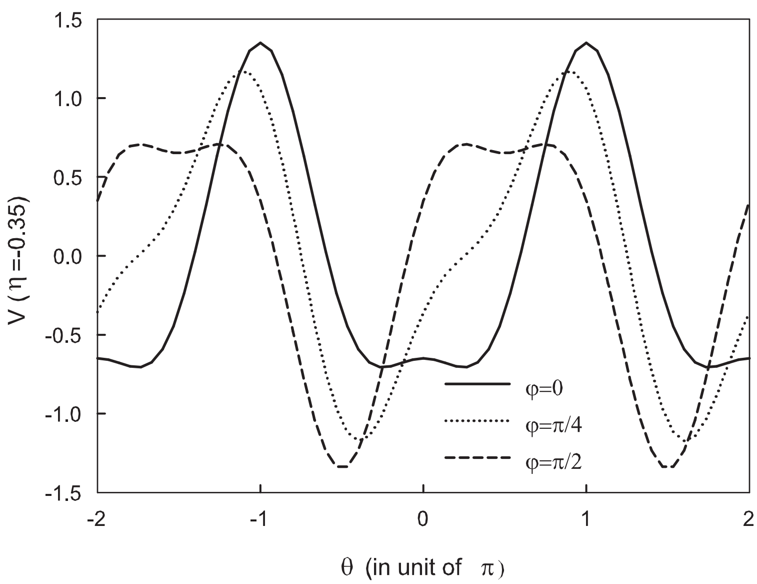
1.5
1.0
0.5
0.0
-0.5
-1.0
-1.5
V (η=-0.35)
-2
-1
0
1
2
θ (in unit of π)
φ=0
φ=π/4
φ=π/2

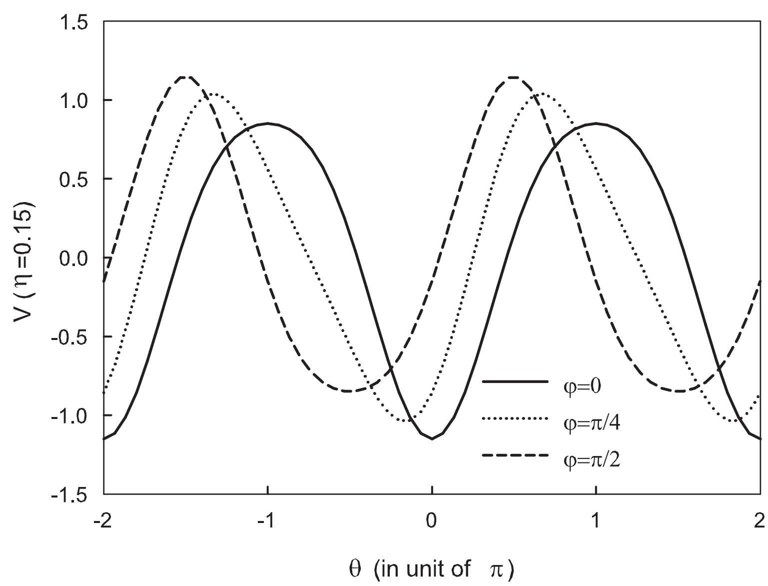
1.5
1.0
0.5
0.0
-0.5
-1.0
-1.5
V (η=0.15)
-2
-1
0
1
2
θ (in unit of π)
φ=0
φ=π/4
φ=π/2

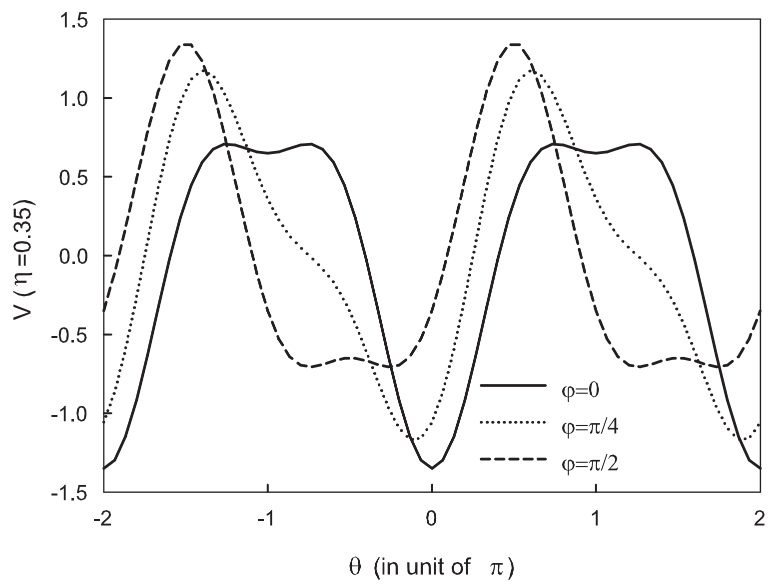

1.5
1.0
0.5
0.0
-0.5
-1.0
-1.5
-2
-1
0
1
2
V (η=0.35)
θ (in unit of π)
φ=0
φ=π/4
φ=π/2

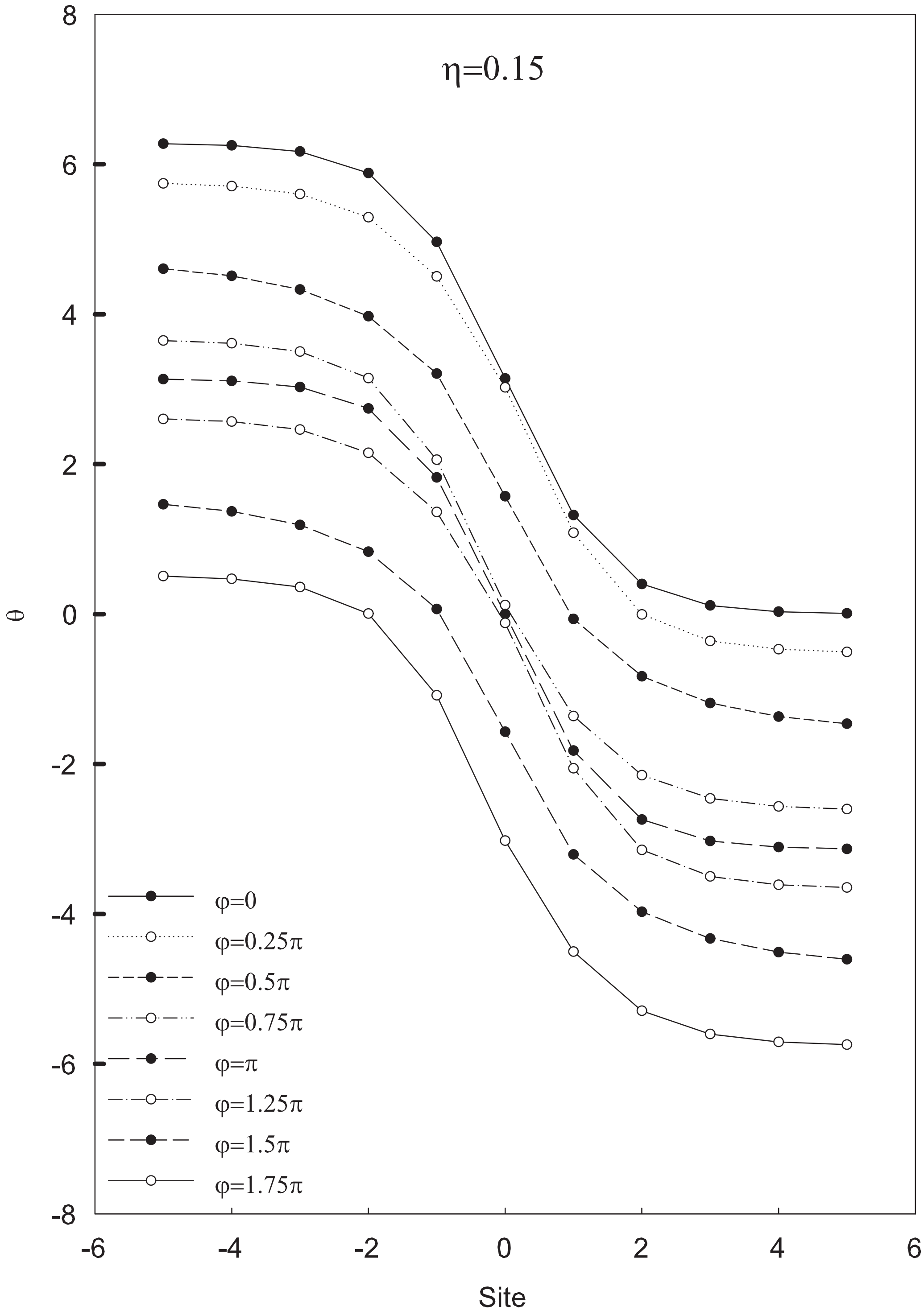
η=0.15
θ
Site
φ=0
φ=0.25π
φ=0.5π
φ=0.75π
φ=π
φ=1.25π
φ=1.5π
φ=1.75π

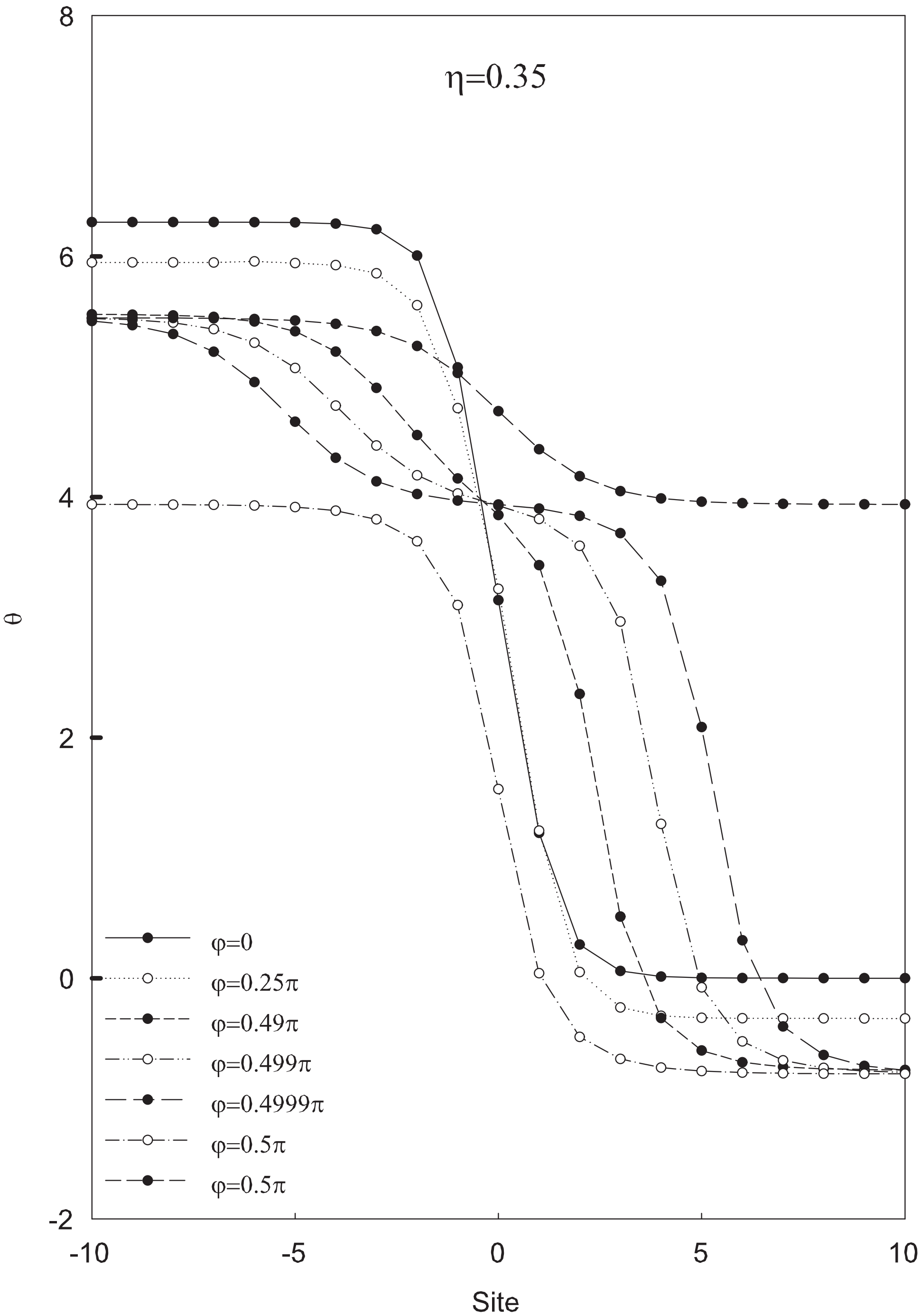
η=0.35
θ
Site
8
6
4
2
0
-2
-10
-5
0
5
10
φ=0
φ=0.25π
φ=0.49π
φ=0.499π
φ=0.4999π
φ=0.5π
φ=0.5π

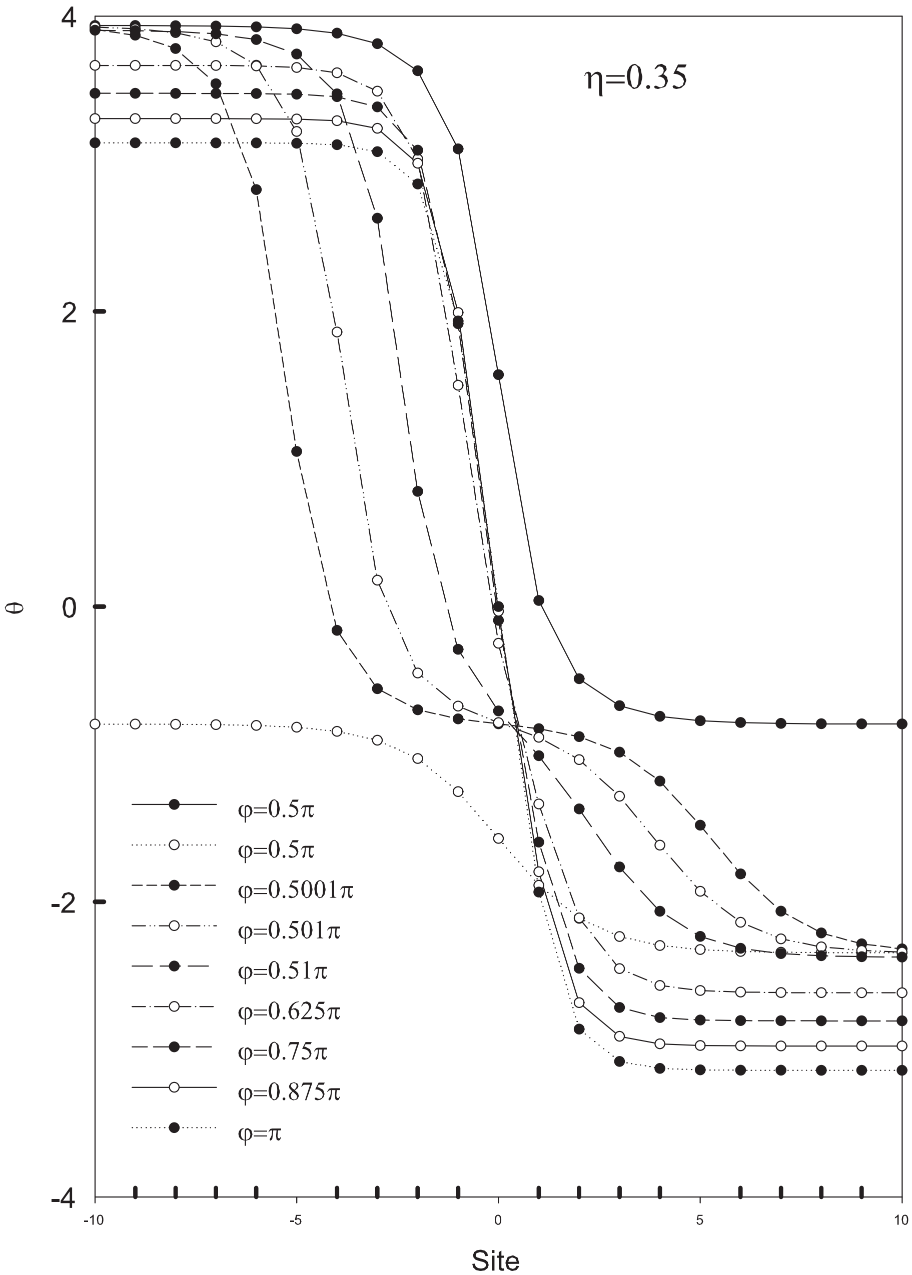

η=0.35
θ
Site
4
2
0
-2
-4
-10
-5
0
5
10
φ=0.5π
φ=0.5π
φ=0.5001π
φ=0.501π
φ=0.51π
φ=0.625π
φ=0.75π
φ=0.875π
φ=π

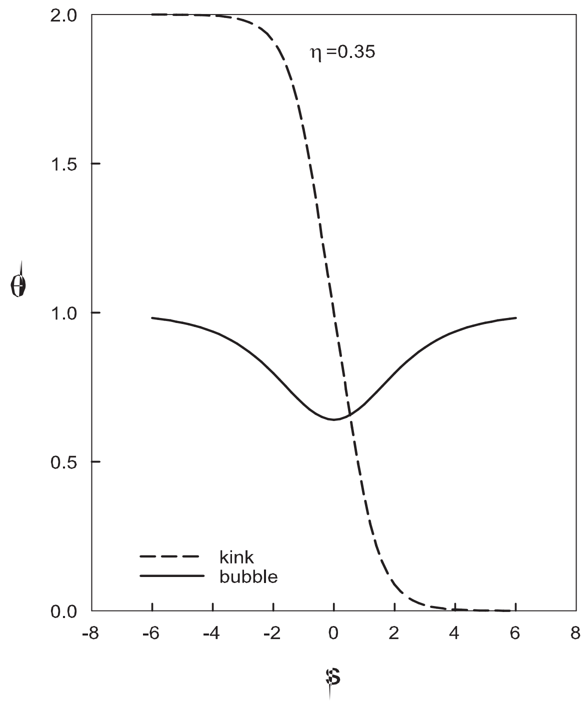
η =0.35
kink
bubble
θ
s
2.0
1.5
1.0
0.5
0.0
-8
-6
-4
-2
0
2
4
6
8

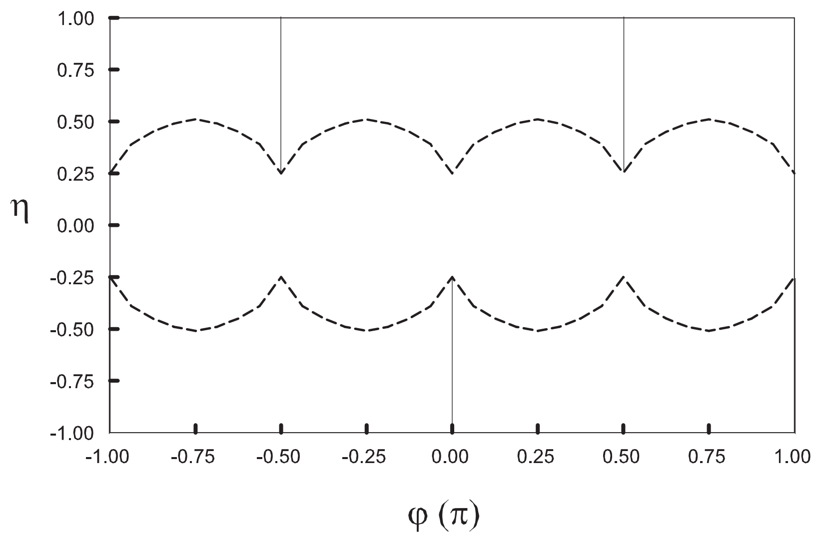
1.00
0.75
0.50
0.25
η
0.00
-0.25
-0.50
-0.75
-1.00
-1.00
-0.75
-0.50
-0.25
0.00
0.25
0.50
0.75
1.00
φ (π)

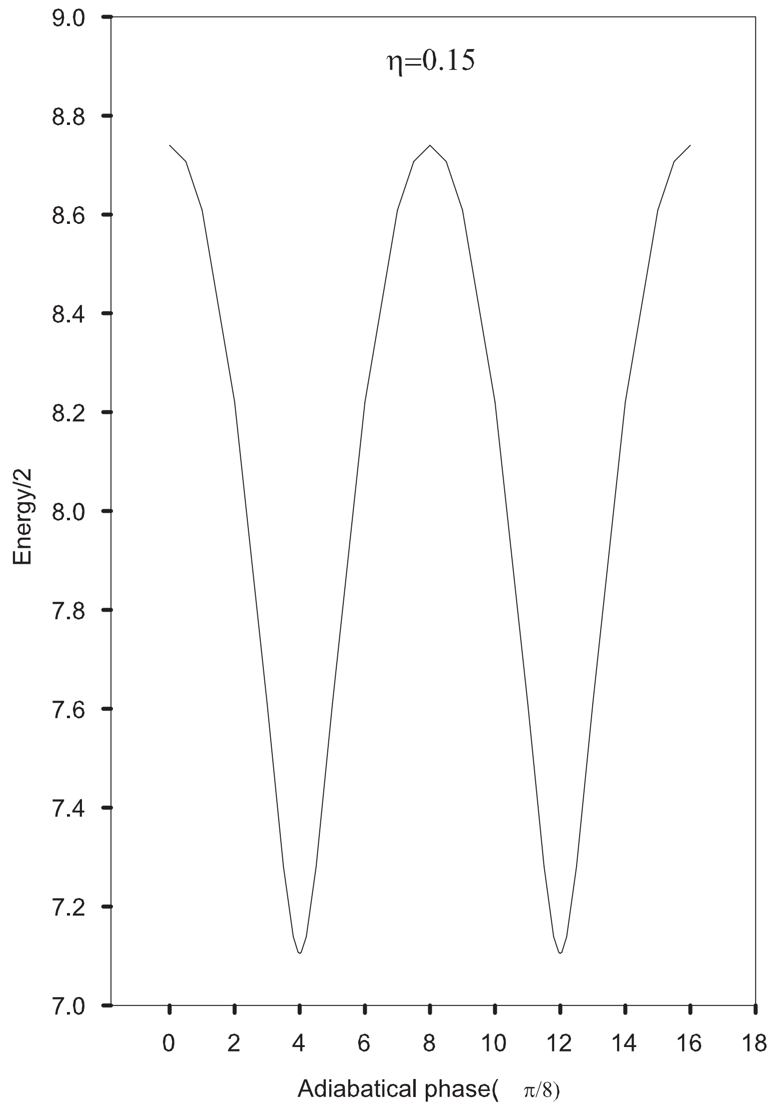
η=0.15
Energy/2
Adiabatical phase(π/8)
9.0
8.8
8.6
8.4
8.2
8.0
7.8
7.6
7.4
7.2
7.0
0
2
4
6
8
10
12
14
16
18

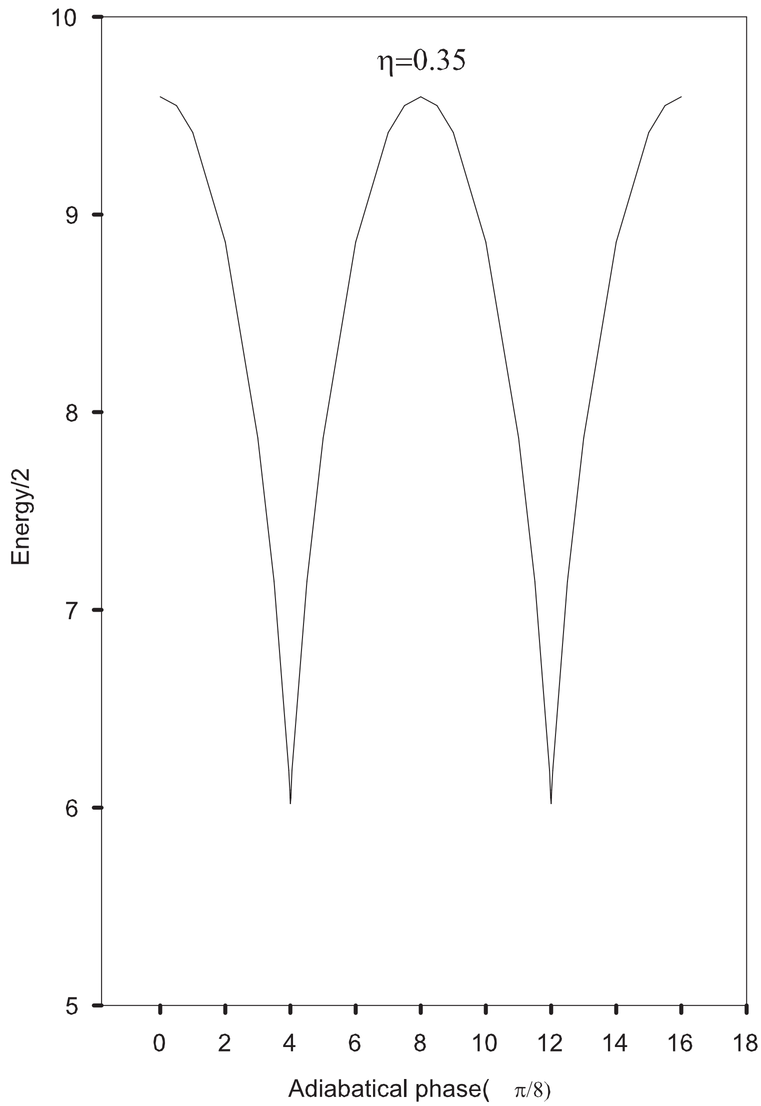

η=0.35
Energy/2
Adiabatical phase(π/8)
10
9
8
7
6
5
0
2
4
6
8
10
12
14
16
18